ChemPubSoc Europe

DOI: 10.1002/chem.201600374

CHEMISTRY
A European Journal
Communication

Spin Crossover

Spectral Signatures of Ultrafast Spin Crossover in Single Crystal $[Fe^{II}(bpy)_3](PF_6)_2$

Ryan Field,[a, b] Lai Chung Liu,[a, b] Wojciech Gawelda,[c] Cheng Lu,[a] and R. J. Dwayne Miller*[a, b]

Abstract: Solvated iron(II)-tris(bipyridine) ($[Fe^{II}(bpy)_3]^{2+}$) has been extensively studied with regard to the spin crossover (SCO) phenomenon. Herein, the ultrafast spin transition dynamics of single crystal $[Fe^{II}(bpy)_3](PF_6)_2$ was characterized for the first time using femtosecond transient absorption (TA) spectroscopy. The single crystal environment is of interest for experiments that probe the nuclear motions involved in the SCO transition, such as femtosecond X-ray and electron diffraction. We found that the TA at early times is very similar to what has been reported in solvated $[Fe^{II}(bpy)_3]^{2+}$, whereas the later dynamics are perturbed in the crystal environment. The lifetime of the high-spin state is found to be much shorter (100 ps) than in solution due to chemical pressure exerted by the lattice. Oscillatory behavior was observed on both time scales. Our results show that single crystal $[Fe^{II}(bpy)_3](PF_6)_2$ serves as an excellent model system for localized molecular spin transitions.

Spin crossover (SCO) is a phenomenon, in which a transition from a low-spin (LS) ground state to a metastable high-spin (HS) excited state is induced by photoexcitation or a change in temperature/pressure.[1,2] Research interest in SCO has been driven by potential applications in magnetic data storage devices and in dye-sensitized solar cells.[3] Additionally, Fe^{II}–polypyridine SCO complexes are known to share a number of photophysical properties with metalloporphyrins, which play a key role in a number of biological processes.[4] Iron(II)–tris(bipyridine) ($[Fe^{II}(bpy)_3]^{2+}$) has been extensively studied with regard to the SCO phenomenon, especially in the aqueous phase.[5–13] Herein, we characterize for the first time the excited-state dynamics of $[Fe^{II}(bpy)_3](PF_6)_2$ single crystals by using femtosecond transient absorption (TA) spectroscopy to elucidate the effects of the single crystal environment. This environment is of particular importance for methods such as femtosecond X-ray and electron diffraction that probe the nuclear motions involved in the spin-transition dynamics and may also provide important insights for applications that require solid-state materials. A number of related compounds have recently been studied in various crystalline states by using ultrafast spectroscopic techniques.[14–18]

In contrast to thermally accessible SCO systems, the LS→HS transition in $[Fe^{II}(bpy)_3]^{2+}$ can only be triggered optically because of a large energy gap between the ground LS state and the lowest-lying HS state (ca. 0.8 eV).[5,6,19] This transition itself is dipole forbidden, and the light-induced SCO proceeds through a relaxation cascade from the dipole-allowed metal-to-ligand charge-transfer (MLCT) states.[3] Although the detailed steps of this relaxation cascade are not entirely settled,[13,20] the general picture that has emerged from studies on the solvated complex is as follows: after excitation to the singlet ^{1}MLCT manifold, the complex relaxes by intersystem crossing (ISC) to a triplet ^{3}MLCT state in <30 fs, from which it decays to the vibrationally hot $^5T_2$ HS state within approximately 150 fs before returning to the ground state on a much longer time scale (ca. 650 ps in room-temperature aqueous solutions).[3,19] A recent optical TA study concluded that the $^5T_2$ state is populated even faster than previously thought (<50 fs).[20] The relaxation into the $^5T_2$ state proceeds with near unity quantum yield and is accompanied by a 0.2 Å elongation of the Fe–N bond.[6,10,21]

In the solvated complex, fast oscillatory signals have been reported in the TA in the UV region near 310 nm, and more recently, in the visible region, overlapping the ground-state bleach (GSB).[7,20,22] These signals have been attributed to wave packets on the nascent formed $^5T_2$ state surface, caused by the driving of specific vibrational modes through the displacive ISC, in which the Fe–N bond rapidly elongates.[7,20] These oscillations appear upon excitation using 580, 530, 400, or 280 nm centered pulses.[7,19,20,22] Because there is a significant energy gap (ca. 1.3 eV) between the minima of the ^{3}MLCT manifold and the $^5T_2$ state, the excess energy following relaxation to the $^5T_2$ state is believed to be converted to vibrational energy, which is dissipated into the caging solvent on the time scale of several picoseconds.[7,20]

Temperature-dependent HS→LS relaxation rates have been previously reported for $[Fe^{II}(bpy)_3]^{2+}$ doped into various isostructural host lattices, $[M(bpy)_3](PF_6)_2$, in which M = Co, Zn,

[a] R. Field, L. C. Liu, Dr. C. Lu, Dr. R. J. D. Miller
Departments of Chemistry and Physics, University of Toronto
80 St. George Street, Toronto, ON M5S 3H6 (Canada)
E-mail: dwayne.miller@mpsd.mpg.de

[b] R. Field, L. C. Liu, Dr. R. J. D. Miller
The Hamburg Centre for Ultrafast Imaging
Centre for Free Electron Laser Science
Max Planck Institute for the Structure and Dynamics of Matter
Bld. 99, Luruper Chaussee 149, 22761 Hamburg (Germany)

[c] Dr. W. Gawelda
European XFEL, Albert-Einstein-Ring 19, 22761 Hamburg (Germany)

Supporting information and the ORCID identification numbers for the authors of this article can be found under http://dx.doi.org/10.1002/chem.201600374.

Mn, and Cd.[23] The driving force for the HS→LS relaxation was found to increase linearly with the decreasing size of the cavity in the host lattice. This destabilizes the HS state, which has an increased volume relative to the LS state. As a consequence, the relaxation rates increase and change over many orders of magnitude as a function of the temperature and the host lattice. The room-temperature HS lifetimes reported in $[Fe^{II}(bpy)_3]^{2+}$ doped into different host crystals all are all in the narrow range of 0.35–2 ns.[23] The influence of the neighboring crystal lattice is called chemical pressure. Despite numerous studies in the solution phase, SCO has never been reported in isolated single crystals of $[Fe^{II}(bpy)_3](PF_6)_2$. This is most likely due to the difficulties associated with studying sufficiently thin crystal samples.

The group velocity dispersion (GVD) corrected TA scans for $[Fe^{II}(bpy)_3](PF_6)_2$ single crystals by using UV and visible continuum probes with 53 fs, 400 nm pump pulses are shown in Figure 1. Parallel pump and probe polarizations were used with the probe polarization set to maximize the absorption of the 533 nm peak. Short (−1–4 ps) and long (4–900 ps) time traces are shown, with 10 fs and 2 ps delay steps, respectively. It should be noted that the UV- and visible-range scans were taken on different samples, which had slightly different thicknesses. As a control experiment, we have also measured aqueous $[Fe^{II}(bpy)_3]^{2+}$ samples under similar excitation conditions (see the Supporting Information). The strong transient signal around time zero is due to cross-phase modulation (CPM).

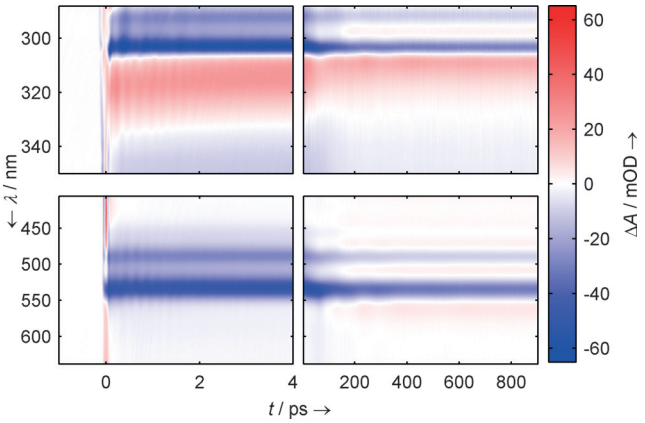

Figure 1. Transient-absorption scans of single crystal $[Fe^{II}(bpy)_3](PF_6)_2$ in the UV (top) and visible (bottom) regions. The occurrence of impulsively excited molecular vibrations are clearly observable at short times, whereas features unique to the single crystal environment are seen on the 100 ps time scale.

On the ultrashort time scale (<5 ps), the measured data is very similar spectrally to what has been observed in solution-phase data.[5,7,20] The visible region is characterized by a short-lived excited-state absorption (ESA) signal at wavelengths <460 and >580 nm, and a persistent GSB across the spectrum. The UV region shows long-lived ESA between 310 and 335 nm, which has been previously attributed to the absorption from the HS state. This ESA undergoes blueshifting on the scale of several picoseconds. Fast oscillations are observed in both the visible and UV regions. These oscillations are significantly different from what has been reported for solvated molecules,[7,20] which we discuss further below. The longer time scale (up to 900 ps) reveals more complicated behavior in the crystalline environment than in the aqueous case. The dynamics cannot be described well as a single exponential decay from the HS state into the ground state. The long-time delay scan also showed strong oscillations with a period on the order of hundreds of picoseconds. These oscillations manifest themselves as oscillations in the spectral peak position, with very little periodic amplitude modulation in the maximum of the peak.

To fit the data, we employ a global-analysis (GA) approach based on singular value decomposition (SVD) of the data. This consists of fitting each of the TA scans using a minimal number of spectral components. Each of the spectral component decays in time as an exponential with a specific lifetime convoluted with the instrument response function. As such, this fit can only model exponential dynamics. Therefore, the oscillatory dynamics and CPM appear in the residuals (Figure S2 in the Supporting Information). To extract the frequencies of the oscillatory components, we apply Fourier analysis to the residuals after $t = 300$ fs. The analytical methods used are described in more detail in the Supporting Information. The resulting fit is shown in Figure 2.

The decay-associated spectra (DAS) and corresponding time constants used in the fit are shown in Figure 3. We caution

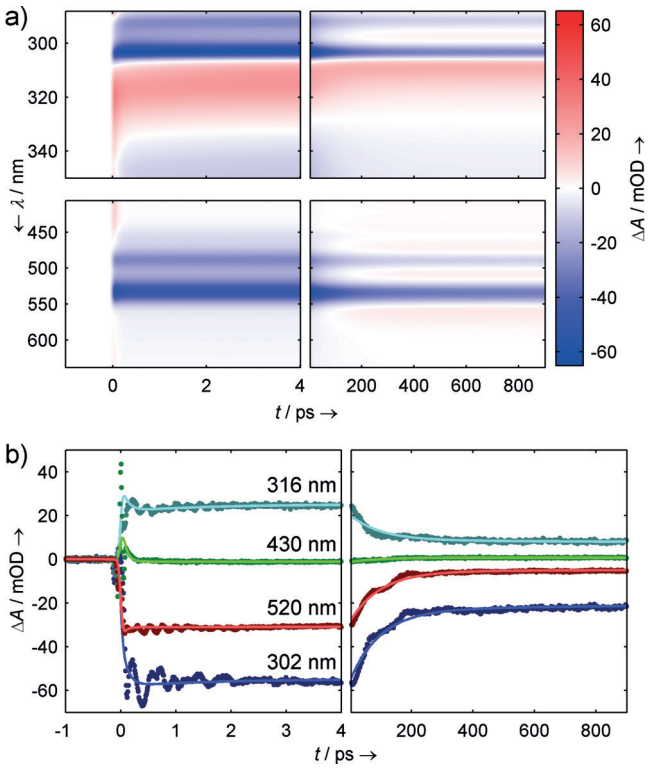

Figure 2. a) Results of the global fit applied to the data presented in Figure 1 in the UV (top) and visible (bottom) ranges. b) Kinetic traces at selected wavelengths. The solid lines overlaid are the fits at these wavelengths.

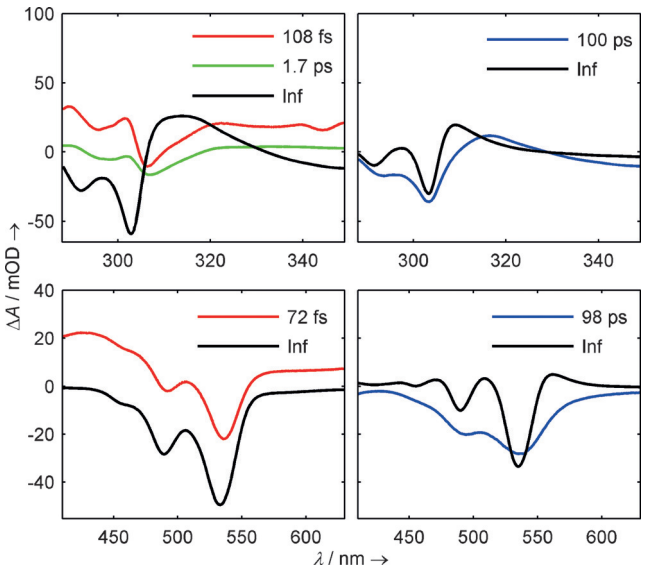

Figure 3. Decay-associated spectra used in the fits shown in Figure 2. The DAS are shown for the short (left) and long (right) time delay scans in the UV (top) and visible (bottom).

that the spectra of the short-lived (ca. 100 fs) components likely have some distortions due to the overlap of the CPM signal and strong initial oscillations.

The short time-delay scan in the visible range was fit with two spectral components. The short-lived component has a lifetime of (72 ± 6) fs, which is comparable to the instrument response time. This component describes the short-lived ESA observed at wavelengths < 460 and > 580 nm, and can be attributed to the decay of the initially excited MLCT states.[5,20] The negative signal between these wavelengths is likely due to crosstalk between the CPM and GSB signals. The second spectral component, which is effectively infinite on this time scale, describes the GSB contribution. In the long time-delay scan, this component is better described by two different spectra. The first, with a lifetime of (98 ± 1) ps, strongly resembles the inverted ground-state absorption (GSA) spectrum and is, therefore, assigned to the HS→LS relaxation within the present picture of the spin dynamics. As was expected due to the crystal packing, the HS state lifetime is roughly an order of magnitude shorter compared to $[Fe^{II}(bpy)_3]^{2+}$ in both CH_3CN (ca. 960 ps) and water (ca. 650 ps).[5,24] The second spectral component, which is effectively infinite on this time scale, is similar to the second derivative of the GSA (Figure S4 in the Supporting Information). Adding this component to the GSA has the effect of slightly lowering the magnitude of the absorption while broadening the absorption peaks. This is most likely the result of transient lattice heating.

The UV short-time delay scan shows two components with time constants similar to those observed in the visible range. The (108 ± 13) fs component can be attributed to the decay of the MLCT state. The slight discrepancy in the duration of this component to that observed in the visible range is likely due to spectral overlap with the strong initial oscillations. The effectively infinite component reflects the superposition of the HS ESA and GSB spectra based on previous assignments of these spectral features. Additionally, a third component, with a time constant of (1.7 ± 0.4) ps, reflects the blueshifting of the HS ESA. Similar-time constants have been used previously to describe vibrational cooling of the HS state in aqueous phase studies,[7,20] which implies that a great deal of excess energy must be dissipated non-radiatively on such a short time scale.[5,20] On the long time scale, the UV data is fitted with two components, time constants of which match well those observed in the visible range. In agreement with those results, the (100 ± 3) ps component can be interpreted as the HS→LS transition, whereas the effectively infinite component describes the effects of lattice heating.

In both the UV and visible ranges probed, the exponential dynamics observed at early times coincide very well to what was observed in the aqueous case. Both environments showed evidence of a sub-100 fs decay of the MLCT state into the HS state, which is then indicated by persistent absorption in the UV range. The vibrational cooling rate of the HS state is identical within error in both environments. The effect of the crystal lattice on these dynamics is only apparent many picoseconds after excitation. This illustrates that the initial MLCT state is localized, with little excitonic coupling between molecules. This result is in contrast to the conclusions of an X-ray powder diffraction study, in which it was argued the initial charge redistribution involves many neighboring unit cells in the single crystal environment.[11] The local nature of the spin transition in crystalline materials has also been evidenced in a number of recent studies on related compounds.[14–17]

The residuals of the fits reveal complex oscillatory dynamics (Figure 4). Four significant frequencies are extracted from the Fourier transform of the early time UV data fit's residuals: (55 ± 7), (81 ± 7), (139 ± 11), and (165 ± 7) cm^{-1}. All of these frequencies were also observed in the visible range (with the extracted frequencies differing by < 2 cm^{-1}), although the signal of the two lower frequencies was close to the noise level. The signal of these two modes was especially strong at wavelengths

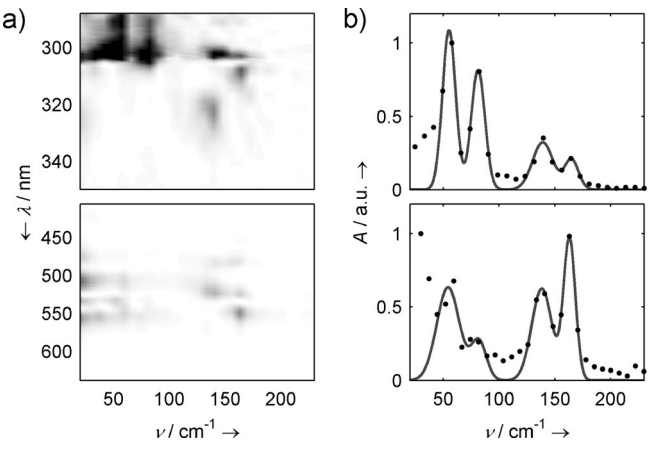

Figure 4. a) Spectrally resolved Fourier transforms of the global fit's residuals after $t = 300$ fs in the UV (top) and visible (bottom) ranges. Both ranges use the same color scale. b) Spectrally integrated Fourier transforms with Gaussian fits in the UV (top) and visible (bottom) ranges.

<308 nm, in which the GSA was dominated by the $\pi\rightarrow\pi^*$ transition on the bipyridine ligands.[20] The two higher frequencies were present in all regions with strong GSB, but also in the HS ESA region. These results are in contrast to our aqueous data, in which a single $(128\pm13)\,cm^{-1}$ frequency was observed (Figure S9 in the Supporting Information). Another study on the solvated complex reported 157 and 220 cm^{-1} modes, in addition to the dominant 128 cm^{-1} mode.[20]

The uncertainty in the extracted frequencies, along with the relatively small number of studies on this aspect of the problem, creates some ambiguity in assigning the modes involved. DFT calculations of the LS $[Fe^{II}(bpy)_3]^{2+}$ complex predicted 140 cm^{-1} and 163 modes corresponding to Fe–N stretching modes, as well as a 61 cm^{-1} mode corresponding to a combination of a N-Fe-N bending mode and a chelate twisting mode, and a 86 cm^{-1} degenerate out-of-plane mode on the bipyridine ligands.[25] Another study calculated 144.6 and 170.2 cm^{-1} Fe–N LS stretching modes in the ground state, but also reported 132.7, 149.6, and 152.4 cm^{-1} HS Fe–N bending modes.[26] Experimental results on a related complex ($[Fe(phen)_2(NCS)_2]$) revealed a number of frequencies in both the LS and HS states within error of those measured in the present study.[27] Of particular interest are 81, 139, and 163 cm^{-1} modes measured in the LS complex, assigned in that study to various bending modes involving the Fe–N bond. There were also 131 and 133 cm^{-1} bending modes observed (by Raman and IR measurements, respectively) in that complex's HS state. In single crystals of the same complex, 85 and 113 cm^{-1} modes were observed in recent femtosecond optical studies.[14,15] Using results obtained by DFT and time-dependent DFT calculations, these modes were assigned to a HS butterfly mode (involving bending of the ligands and N-Fe-N angles) and a totally symmetric HS Fe–N stretching mode, respectively.[15]

In the present study, the oscillatory dynamics were measured in both the aqueous and crystalline phases, showing that the dominant modes involved in the dynamics are not the same. In the aqueous complex, the symmetric Fe–N stretching mode (128 cm^{-1}) is the strongest one observed, in agreement with previous studies.[7,20] The $[Fe^{II}(bpy)_3](PF_6)_2$ single crystal exhibits more complicated structural distortions, involving ligand bending and twisting modes, mixed with the Fe–N stretching. This effect is most probably another consequence of the dense crystal packing in the single crystal environment. Given our observations, along with the available literature, the most likely conclusion is that the oscillations observed are primarily due to impulsively stimulated Raman modes on the LS surface. Within our margin of error, the 139 cm^{-1} mode could be assigned to an HS bending mode. The excitation of such a mode would be expected to be delayed, because the time scale involved in the LS$\rightarrow$HS transition, observable as a phase shift relative to impulsively excited Raman modes on the ground state surface. A slight phase shift was observed between the 139 cm^{-1} mode observed in the GSB and that observed in the HS ESA, though this was not clearly resolvable because of overlap with the 165 cm^{-1} mode in the GSB region.

Slow oscillations with periods on the order of hundreds of picoseconds were observed in the long-time delay scans. A crystal-thickness dependence was conducted, and a linear correlation was found between the optical density (and therefore thickness) of the crystal samples at 533 nm and the period of the oscillations (Figure S3 in the Supporting Information). Therefore, these oscillations can be simply explained as the excitation of an acoustic phonon driven by thermal expansion and subject to the boundary conditions defined by the crystal thickness. The speed of sound implied by the measured periods and crystal thicknesses is $(2.7\pm0.2)\,km\,s^{-1}$, which is in good agreement with typical values observed in molecular crystals. This acoustic (or density) induced modulation of the spectrum gives a direct observation of the electron–phonon coupling in this system. This feature is generally not observed in solid-state systems and usually requires going to very low temperatures to sufficiently narrow the absorption line shapes to observe the otherwise very small acoustic modulation of the spectral energy levels.[28,29] This observation indicates that there is very strong electron–phonon coupling in this system.

We have characterized the ultrafast dynamics of $[Fe^{II}(bpy)_3](PF_6)_2$ single crystals in the UV and visible ranges. At early times, the exponential dynamics and spectral features observed were fully analogous to what has been previously observed in aqueous $[Fe^{II}(bpy)_3]^{2+}$. However, the complex oscillatory dynamics revealed that the dominant modes involved in the early dynamics are significantly different. Longer time scales showed more complicated dynamics than in the solvated case, resulting from collective lattice effects. We have determined the lifetime of the lowest-lying HS state based on previous spectral assignments of the spin states to be reduced to approximately 100 ps, thus significantly shorter than in solution phase, due to the chemical pressure exerted by the nearest neighbors.[23] The initially excited MLCT state is well defined as a localized transition very similar to that found in solution. The fact that the exponential dynamics at early times are nearly identical to those found in aqueous studies illustrates that there are little excitonic or collective excitations even within the confines of a pure single crystal. As a consequence, single crystal studies of $[Fe^{II}(bpy)_3](PF_6)_2$ provide an excellent model system for understanding MLCT, and how this change in charge distribution apparently leads to such an exceptionally fast spin transition in this system. The use of structural probes, such as femtosecond X-ray and electron diffraction, will elucidate the nuclear motions involved. These motions ultimately must lead to a fluctuating magnetic dipole moment that in turn couples the spin states between electronic manifolds. Understanding this process will help to control and further develop molecular spin systems.

Experimental Section

Thin slices of $[Fe^{II}(bpy)_3](PF_6)_2$ single crystal with varying thickness (ca. 100–300 nm) were microtomed from bulk crystal samples along the (210) plane and mounted on 0.5 mm thick sapphire substrates for measurement. TA was probed in the visible and UV ranges using white-light continua seeded with 800 and 400 nm centered pulses, respectively. 53 fs pulses centered at 400 nm were used to excite the sample, with a fluence of approximately

3 mJ cm^{-2} (ca. 57 GW cm^{-2}) at the sample position. Parallel pump and probe polarizations were used with the probe polarization set to maximize the sample absorption at 533 nm. Further experimental details are given in the Supporting Information.

Acknowledgements

This work was funded by the Max Planck Society in collaboration with the Centre for Free Electron Laser Science and the Hamburg Centre for Ultrafast Imaging (University of Hamburg). L.L. acknowledges funding from the Natural Sciences and Engineering Research Council of Canada (NSERC). W.G. acknowledges funding by the European XFEL and further financial support from the Deutsche Forschungsgemeinschaft (via SFB925, TPA4) and the Hamburg Centre for Ultrafast Imaging. The authors thank Christian Bressler for comments on the manuscript in relation to previous work. R.F. would like to thank Valentyn Prokhorenko for support throughout the development of the experimental apparatus.

Keywords: charge transfer · electron-phonon coupling · iron · spin crossover · time-resolved spectroscopy

[1] P. Gütlich, A. B. Gaspar, Y. Garcia, *Beilstein J. Org. Chem.* **2013**, *9*, 342.
[2] A. Hauser in *Spin Crossover in Transition Metal Compounds II* (Eds.: P. Gütlich, H. A. Goodwin), Springer, Heidelberg, **2004**, pp. 155 – 198.
[3] A. Cannizzo, C. J. Milne, C. Consani, W. Gawelda, C. Bressler, F. van Mourik, M. Chergui, *Coord. Chem. Rev.* **2010**, *254*, 2677.
[4] M. Chergui in *In-situ Materials Characterization* (Eds.: A. Ziegler, H. Graafsma, X. F. Zhang, J. W. M. Frenken), Springer, Heidelberg, **2014**, pp. 1 – 38.
[5] W. Gawelda, A. Cannizzo, V. T. Pham, F. van Mourik, C. Bressler, M. Chergui, *J. Am. Chem. Soc.* **2007**, *129*, 8199.
[6] W. Gawelda, V. T. Pham, M. Benfatto, Y. Zaushit *syn*, M. Kaiser, D. Grolimund, S. L. Johnson, R. Abela, A. Hauser, C. Bressler, M. Chergui, *Phys. Rev. Lett.* **2007**, 98, 057401.
[7] C. Consani, M. Prémont-Schwarz, A. ElNahhas, C. Bressler, F. van Mourik, A. Cannizzo, M. Chergui, *Angew. Chem. Int. Ed.* **2009**, *48*, 7184; *Angew. Chem.* **2009**, *121*, 7320.
[8] A. Vargas, A. Hauser, L. M. L. Daku, *J. Chem. Theory Comput.* **2009**, *5*, 97.
[9] C. de Graaf, C. Sousa, *Chem. Eur. J.* **2010**, *16*, 4550.
[10] C. Bressler, C. Milne, V. T. Pham, A. ElNahhas, R. M. van der Veen, W. Gawelda, S. Johnson, P. Beaud, D. Grolimund, M. Kaiser, C. N. Borca, G. Ingold, R. Abela, M. Chergui, *Science* **2009**, *323*, 489.
[11] B. Freyer, F. Zamponi, V. Juvé, J. Stingl, M. Woerner, T. Elsaesser, M. Chergui, *J. Chem. Phys.* **2013**, *138*, 144504.
[12] H. T. Lemke, C. Bressler, L. X. Chen, D. M. Fritz, K. J. Gaffney, A. Galler, W. Gawelda, K. Haldrup, R. W. Hartsock, H. Ihee, J. Kim, K. H. Kim, J. H. Lee, M. M. Nielsen, A. B. Stickrath, W. Zhang, D. Zhu and M. Cammarata, *J. Phys. Chem. A* **2013**, *117*, 735.
[13] W. Zhang, R. A. Mori, U. Bergmann, C. Bressler, M. Chollet, A. Galler, W. Gawelda, R. G. Hadt, R. W. Hartsock, T. Kroll, K. S. Kjær, K. Kubiček, H. T. Lemke, H. W. Liang, D. A. Meyer, M. M. Nielsen, C. Purser, J. S. Robinson, E. I. Solomon, Z. Sun, D. Sokaras, T. B. van Driel, G. Vankó, T. C. Weng, D. Zhu, K. J. Gaffney, *Nature* **2014**, *509*, 345.
[14] M. Cammarata, R. Bertoni, M. Lorenc, H. Cailleau, S. Di Matteo, C. Mauriac, S. F. Matar, H. Lemke, M. Chollet, S. Ravy, C. Laulhé, J. F. Létard, E. Collet, *Phys. Rev. Lett.* **2014**, *113*, 227402.
[15] R. Bertoni, M. Cammarata, M. Lorenc, S. F. Matar, J. F. Létard, H. T. Lemke, E. Collet, *Acc. Chem. Res.* **2015**, *48*, 774.
[16] R. Bertoni, M. Lorenc, A. Tissot, M. Servol, M. L. Boillot, E. Collet, *Angew. Chem. Int. Ed.* **2012**, *51*, 7485; *Angew. Chem.* **2012**, *124*, 7603.
[17] R. Bertoni, M. Lorenc, J. Laisney, A. Tissot, A. Moréac, S. F. Matar, M. L. Boillot, *J. Mater. Chem. C* **2015**, *3*, 7792.
[18] A. Marino, P. Chakraborty, M. Servol, M. Lorenc, E. Collet, A. Hauser, *Angew. Chem. Int. Ed.* **2014**, *53*, 3863; *Angew. Chem.* **2014**, *126*, 3944.
[19] M. Chergui, *Dalton Trans.* **2012**, *41*, 13022.
[20] G. Auböck, M. Chergui, *Nat. Chem.* **2015**, *7*, 629.
[21] M. A. Bergkamp, C. K. Chang, T. L. J. Netzel, *J. Phys. Chem.* **1983**, *87*, 4441.
[22] G. Auböck, C. Consani, R. Monni, A. Cannizzo, F. van Mourik, M. Chergui, *Rev. Sci. Instrum.* **2012**, *83*, 093105.
[23] A. Hauser, N. Amstutz, S. Delahaye, A. Sadki, S. Schenker, R. Sieber, M. Zerara, *Chimia* **2002**, *56*, 685.
[24] L. L. Jamula, A. M. Brown, D. Guo, J. K. McCusker, *Inorg. Chem.* **2014**, *53*, 15.
[25] B. D. Alexander, T. J. Dines, R. W. Longhurst, *Chem. Phys.* **2008**, *352*, 19.
[26] C. Sousa, C. Graaf, A. Rudavskyi, R. Broer, J. Tatchen, M. Etinski, C. M. Marian, *Chem. Eur. J.* **2013**, *19*, 17541.
[27] K. L. Ronayne, H. Paulsen, A. Höfer, A. C. Dennis, J. A. Wolny, A. I. Chumakov, V. Schünemann, H. Winkler, H. Spiering, A. Bousseksou, P. Gütlich, A. X. Trautwein, J. J. McGarvey, *Phys. Chem. Chem. Phys.* **2006**, *8*, 4685.
[28] R. J. D. Miller, M. Pierre, T. S. Rose, M. D. Fayer, *J. Phys. Chem.* **1984**, *88*, 3021.
[29] K. A. Nelson, R. Casalegno, R. J. D. Miller, M. D. Fayer, *J. Chem. Phys.* **1982**, *77*, 1144.

Received: January 27, 2016
Published online on February 25, 2016